Green fabrication of (6,5)CNT/protein transistor endowed with specific recognition

Marcello Berto, Matteo Di Giosia, Martina Giordani, Matteo Sensi, Francesco Valle, Andrea Alessandrini, Claudia Menozzi, Andrea Cantelli, G. Carlo Gazzadi, Francesco Zerbetto, Matteo Calvaresi, Fabio Biscarini and Carlo A. Bortolotti**

Dr. M. Berto, Dr. M. Giordani, Dr. M. Sensi, Prof. F. Biscarini, Dr. C.A. Bortolotti
Dipartimento di Scienze della Vita - Università di Modena e Reggio Emilia, Via Campi 103, Modena 41125, Italy
Email: carloaugusto.bortolotti@unimore.it

Dr. Matteo Di Giosia, Dr. A. Cantelli, Prof. Francesco Zerbetto, Prof. Matteo Calvaresi
Dipartimento di Chimica "Giacomo Ciamician", Alma Mater Studiorum - Università di Bologna, Via Francesco Selmi 2, 40126 Bologna, Italy
Email: matteo.calvaresi3@unibo.it

Dr. F. Valle
CNR - Istituto per lo Studio di Materiali Nanostrutturati, Via P. Gobetti, 101, 40129, Bologna, Italy

Dr. F. Valle
Consorzio Interuniversitario per lo Sviluppo dei Sistemi a Grande Interfase (CSGI), via della Lastruccia 3, 50019 Firenze, Italy

Prof. A. Alessandrini, Dr. C. Menozzi, Dr. G.C. Gazzadi
CNR - Istituto Nanoscienze, S3, Via Campi 213/A, 41125, Modena, Italy

Prof. A. Alessandrini, Dr. C. Menozzi
Dipartimento di Science Fisiche, Informatiche e Matematiche, Università di Modena e Reggio Emilia, Via Campi 213/A, 41125, Modena, Italy

Prof. F. Biscarini
Center for Translational Neurophysiology - Istituto Italiano di Tecnologia
Via Fossato di Mortara 17-19, Ferrara 44100, Italy

Keywords: carbon nanotubes, lysozyme, EGT, biosensor, green chemistry

ABSTRACT

A general single-step approach is introduced for the green fabrication of hybrid biosensors from water dispersion. The resulting device integrates the semiconducting properties of a CNT and the functionality of a protein. In the initial aqueous phase, the protein (viz., lysozyme) disperses the (6,5) CNT. Drop-casting of the dispersion on a test pattern (a silicon wafer with interdigitated Au source and drain electrodes yields a fully-operating, robust, electrolyte-gated transistor (EGT) in one step. The EGT response to biorecognition is then assessed using the lysozyme inhibitor N-acetyl glucosamine trisaccharide. Analysis of the output signal allows us to extract a protein-substrate binding constant in line with values reported for the free (without CNT) system. The methodology is robust, easy to optimize, re-directable towards different targets and sets the grounds for a new class of CNT-protein biosensors that overcome many limitations of the technology of fabrication of CNT biosensors.

1. Introduction

Bioelectronics links bio-based signals and electronics by means of transducers units. Commercially available examples of bioelectronic devices include blood glucose sensors, deep-brain stimulators, neural prosthetics, and cardiac pacemakers.[1–4] The decrease of the size and physical dimension of the transducers will attenuate their invasiveness, yielding a reduced reaction of the living organism against a foreign object the enhancement of the signal-to-noise ratio, and higher spatio-temporal resolution. The ultimate progress from bioelectronics to nano-bioelectronics[5,6] will exploit nanowires, low dimensional materials, and nanostructured carbon allotropes such as Carbon Nanotubes (CNT). These promising candidates for high performing transducers are characterized by outstanding electronic properties.[7–17] In particular, the interest for CNTs as biosensor components[18–26] is further supported by their exceptional electrical performances, even at small applied potentials (< 1V). CNT-field-effect transistor-based biosensors have shown great potential for ultrasensitive biomarker detection despite the presence of important challenges, which include difficulty in stable functionalization, incompatibility with scalable fabrication, and nonuniform performance.[27] A crucial challenge lies in the CNTs insolubility both in water and in organic solvents and in their high tendency to aggregate that hinder their wide applicability. Methods enabling their processability are strongly needed.

Carbon nanotubes are dispersed either mechanically or chemically. The direct “mechanical” methods tend to have low efficiency and to yield poor stability of the dispersion. The “chemical” covalent approach functionalizes the CNT walls with chemical moieties. It improves solubility in solvents and reduces the tendency to aggregate,[28] but it remains an aggressive methodology prone to cause defects on the CNT walls that can ultimately modify their peculiar electrical properties, which are essential for their applications in FET technology. Of these approaches, the noncovalent functionalization is particularly attractive since it preserves the characteristic electronic properties

of the CNT and can exploit a variety of molecules such as surfactants, polymers and biomolecules.[29–33]

The technological shift from transducers to biosensors requires the integration of a specific recognition unit in the electronic transducer that, in the case of CNT-based biosensors, may follow different alternatives such as covalent attachment (tethering),[34] non-covalent adsorption using linker molecules,[35,36] direct adsorption via hydrophobic or electrostatic interactions with the tube surface[31,37,38] or entrapment in a polymeric matrix.[39]

In this work, we use a protein, namely lysozyme, as dispersant agent for a selected CNT, the semiconducting single wall (6,5)CNT.[40] The use of lysozyme (LZ) improves the green ~~enables~~ processability of the (6,5)CNT, without the need of organic solvents to process and deposit the CNT.[41] At the same time it introduces the protein directly on the semiconducting surface:[42] the wild type protein can be used directly without the use of tethering groups[41] or the need of covalent functionalization of the tube surface.[43]

This approach produces a highly stable hybrid characterized by a large interaction energy between CNT and protein.[44] Yet, it retains the electronic properties of the CNT and the full protein functionality.[45] The procedure proposed here (a) affords green water-processing of the system to produce an Electrolyte-Gated Transistor (EGT) and (b) endows the (6,5)CNT-based active channel with the additional functionality of biorecognition. The LZ/(6,5)CNT hybrid works both as a semiconductor layer and as a recognition element. The device is fabricated by a one-step self-organized process[46] and overcomes several severe limitations that exist in the present technology for the fabrication of robust CNT transistors. The proposed strategy allows to deposit the semiconductive channel in a fast, easy and more green way directly from aqueous solution, while most of the CNT-based transistors described in previous works require organic solvents,[41,47] the

application of external electrical potential to orientate the carbon nanotubes during the deposition,[41,47] or the use of specific fabrication techniques such as chemical vapor deposition or spray-coating.[43,46]

2. Results and discussion

LZ/(6,5)CNT hybrids were synthesized by ultrasonication of (6,5)CNT powder in an aqueous solution of lysozyme.[48,49] The solution was centrifuged and the supernatant was collected. The UV–vis spectrum of LZ/(6,5)CNT showed a band centered at 280 nm, typical of the protein, and the E11 and E22 transitions of the (6,5)CNTs (**Figure S1a**). (6,5)CNTs are dominant in the sample. It is well established that only debundled CNTs exhibit well-defined peaks in the Vis-NIR region due to the van Hove transitions.[50–52]

Atomic force microscopy (AFM) images (**Figure S2a**) of the deposited LZ/(6,5)CNT hybrids are a clear evidence of the presence of highly dispersed and debundled LZ/(6,5)CNT adducts in the aqueous systems. The profile analysis of lysozyme-(6,5)CNT (Figures S3a and S3b), clearly shows the dispersion of 0.78 nm diameter (6,5)CNTs, and the presence of lysozyme surrounding the tube (Figures S3c and Figure S3d). In the magnification of **Figure S3,** it is possible to recognize the lysozyme astride the (6,5)CNTs.

Electrolyte-gated transistors were first fabricated by drop casting of a 150 μg/ml aqueous solution of LZ/(6,5)CNT hybrids on a silicon substrate to bridge the interdigitated Au source and drain electrodes (width/length ratio, W/L, is 560) (**Figure 1a**). The channel formed by the randomly oriented LZ/(6,5)CNT hybrids network is gated by a Pt wire immersed in 50 mM PBS.

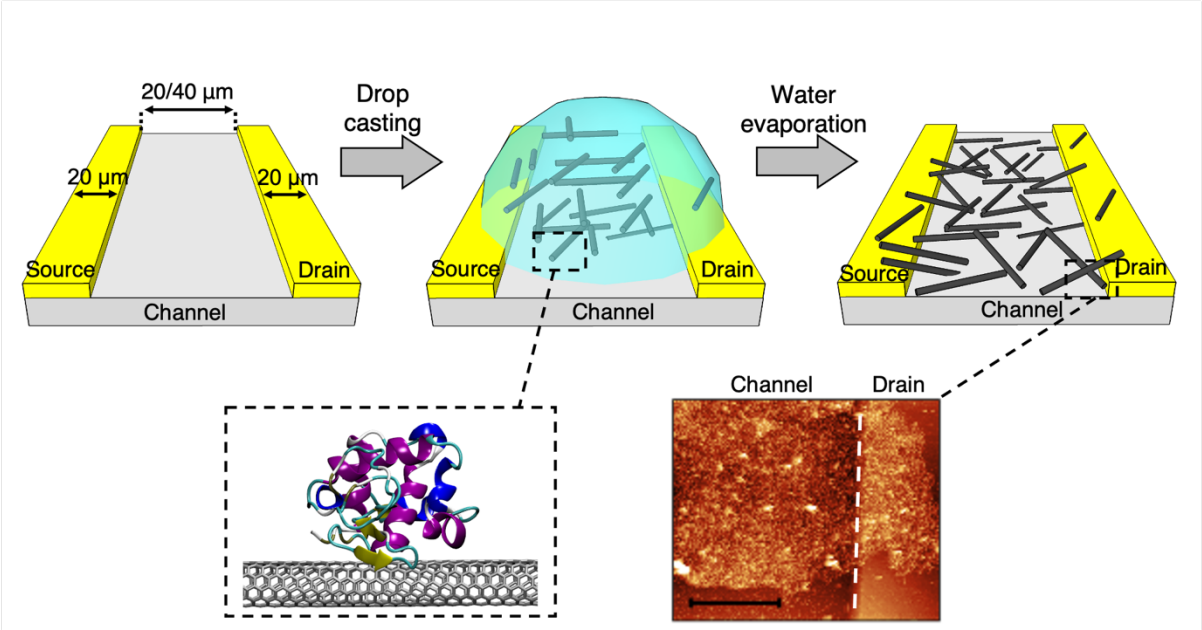

Figure 1. Fabrication procedure of LZ/(6,5)CNT-based EGTs: (top) from left to right, deposition by drop casting of the LZ/(6,5)CNT water dispersion on a clean silicon wafer surface; after water evaporation, few nanotubes bundled are present on the surface (average CNT length = 1 µm); (bottom) in the left panel, one of the potential interaction geometries between a lysozyme molecule and a (6,5)CNT is schematically depicted; in the right panel, AFM image of LZ/(6,5)CNT bundles (the bar corresponds to 5 µm).

Figure 2a and **Figure 2b** show the typical output and transfer characteristics of a p-type semiconductor, with the drain current increasing as V_{GS} becomes more negative. In particular, Fig. 2a displays I_{DS} vs. V_{DS}, at constant V_{GS} values in the 0 ÷ -0.5 V range; Fig. 2b presents I_{DS} vs. V_{GS}, at constant V_{DS} = -0.1 V. Importantly, (6,5)CNTs from the same batch dispersed with the surfactant SDS (sodium dodecyl sulphate) and drop-cast on same test patterns do not exhibit current modulation in the same voltage range of the gate (**Figure S4**). Atomic Force Microscopy characterization of the SDS/(6,5)CNTs dispersion revealed that it is mainly characterized by

bundles and ropes (Figure S2b). The bundling of the semiconducting (6,5)CNT to ropes is known to result in a decrease of the energy gap[53] and in the appearance of metallicity character, as confirmed here by electrical measurements on SDS/(6,5)CNTs EGT. The control experiment with SDS/(6,5)CNTs suggests that LZ is a more effective dispersant agent for (6,5)CNT than SDS, and that the use of LZ as dispersant fully preserves the semiconducting character of (6,5)CNTs.

Two issues emerge from these data:

1) The SDS molecules adsorb non-specifically on the tube surface with the appearance of bundling and roping. The shape-complementarity interaction between LZ and carbon nanotubes disperses them monomolecularly, preserving their electronic properties.[38,44]
2) The micelles of SDS disperses the metallic catalyst particles that are inevitably present in the CNT sample.[54] On the contrary, lysozyme, for geometric reasons, is selective only for the CNTs. The electronic properties of CNTs are affected by the presence of the metal particles that have been responsible for hindering the development of CNT transistors.[54]

The electrical response of the LZ/CNT EGT to the field effect is ascribed to ions migration forming electrical double layers at the gate/electrolyte and electrolyte/ LZ/CNT interfaces. The current modulation arises from a change of the electronic charge density within the semiconducting material. The saturation current in Figure 2a is reached at relatively low drain voltages (around -0.25 V). The LZ/(6,5)CNT EGTs exhibit optimal operation, as witnessed by the almost negligible hysteresis (Figure 2b) and by the average threshold voltage, V_{th} = -331 (±10) mV, the latter value ensures operation at low biasing voltages. To assess the robustness of the device response, eight different LZ/(6,5)CNT EGTs were fabricated and their transfer characteristics were measured. Figure 2c shows the average transfer curves: the fabrication procedure shows remarkably high

reproducibility, which is one of the advantages of the use of networks made by a selected CNT over single tube devices that are prone to sizable fluctuations because of the nature of the channel based on an individual CNT.[19] These findings indicate that the protein dispersion is able to overcome two recurrent issues, i.e. i) high tendency of the CNT to aggregate, forming bundles and ropes that degrade their semiconducting characteristics, and ii) the scarce stability of CNTs in transistors, affecting the electrical response of solution-processed (6,5)CNTs.[55]

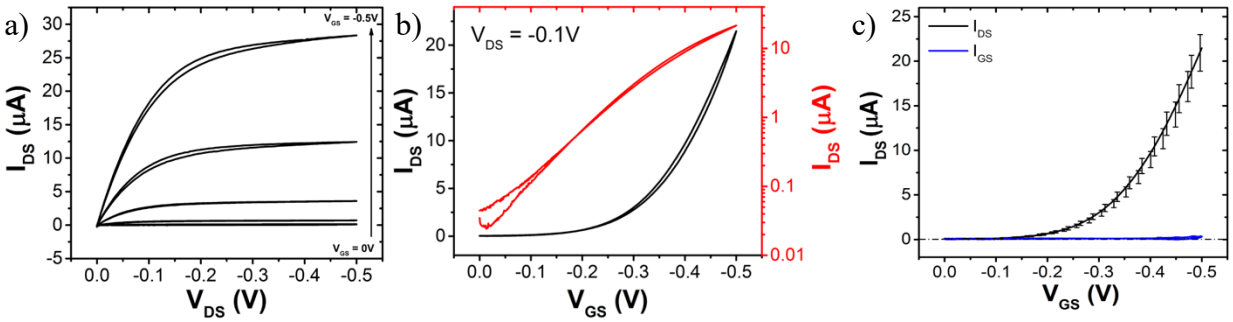

Figure 2. Electrical performance of LZ/(6,5)CNT EGT. (a) output characteristics recorded for I_{GS} = 0V ÷ -0.5V; (b) lin-lin (black) and semilog (red) transfer characteristics; (c) average transfers characteristics recorded at V_{DS} = -0.1 V; in black the channel current I_{DS}, in blue the leakage current I_{GS}. Error bars correspond to the rms of the current averaged over eight devices.

The average transconductance g_m is 137 (±4) μS and the on/off ratio is about 778. The moderate on/off ratio can be ascribed to high off-current values as shown in Figure 2b, which can result either from the presence of a residual small population of metallic tubes in the channel or from sizable leakage currents arising from the exposure of the source electrode to the electrolyte (see Figure 1c). The latter factor, due to low CNT coverage on electrodes, would be however common to all CNTs transistors.[12,18] We assessed the possibility of depositing a semiconducting LZ/(6,5)CNT channel from a more diluted solution: we could obtain a working transistor using a LZ/(6,5)CNT concentration as low as 1.5 μg/ml, while lower concentrations did not yield

semiconducting channel, most likely because of the fact that continuous pathways bridging source and drain were not connected as a consequence of the low density that is apparently below the percolation threshold.[56] The electrical performances of the CNT EGTs fabricated by drop casting of a 1.5 μg/ml solution are in line with other reported semiconducting (6,5)CNT field-effect transistors,[18,55] though worse than those obtained from the 100-times more concentrated hybrid CNT/protein solution, as reported in **Table S1** and **Figure S5 and Figure S6**.

In order to test the possibility of translating our fabrication procedure to a different, widely used, substrate, we deposited 1.50 μg/ml LZ/(6,5)CNT solution on quartz, instead of the Si wafer, with Au source and drain interdigitated electrodes (see **Figure S7**). Interestingly, the same protocol yields semiconducting LZ/(6,5)CNT channels also on a different, widely used substrate. The performances of Si-based and quartz-based devices are comparable, as reported in **Table S1**.

We rationalize the differences of the electrical performances between the devices prepared from 1.5 μg/ml solution and 150 μg/ml solution in terms of morphology of the semiconductive film. In our devices, charge transport (hence output current, on/off ratio and transconductance) relies on the LZ/(6,5)CNT percolation network connecting source and drain electrodes. Atomic force microscopy (AFM) (Figure 1) shows that the channel consists of a dense network of LZ/(6,5)CNT, that covers only a limited area of the channel. Source and drain electrodes are partially covered by LZ/(6,5)CNT, while most of their area is left bare, thus in direct contact with the electrolyte. This is observed at both concentrations. This situation will affect charge injection as well as the effective W/L ratio of the transistor characteristics. We infer that both concentrations are well above percolation threshold, the most influential factor will be the effective width. This is confirmed by the morphology of LZ/(6,5)CNT percolation networks measured by Scanning Electron

Microscopy (SEM) as shown in **Figure 3**. The SEM images and their Power Spectral Density Function (PSDF) analysis show that, despite the different initial concentration of LZ(6,5)CNT solution, the resulting bundles are characterized by a similar porous morphology. The PSDF spectra for both concentrations are very similar, in particular the bending of the initial plateau towards a linear self-affine dependence takes place at the same values of k, corresponding to a characteristic length of about 40 nm, that can be associated to the average pore diameter observed in Figures 3a and 3b. Despite the fact that topography is indirectly embedded in the intensity of the signal, which makes the consideration by and large qualitative, the PSDs hint to a greater roughness, and hence thickness, of the deposit from the more concentrated solution. This is confirmed by the measurement of thickness of LZ/(6,5)CNT bundles (Figure 3c) from SEM cross-sections: bundles formed from the more concentrated solution are thicker (141 ± 57 nm), conversely those from the less concentrated solution are thinner and more homogeneous (42 ± 19 nm). The scaling of the transconductance (see Table 1) mirrors the thickness increase of the film with the concentration. This bears similarity with the observed behavior of conductive polymers, such as PEDOT:PSS in organic electrochemical transistors, whose porous morphology is associated to the so-called volumetric capacitance.[57,58]

As can be observed from the transfer curves (semilog format) in Figure 2b, the higher on/off ratio is mostly caused by the lowering of the off-current (more than five times smaller) with respect to the enhancement of the maximum current (about twice).

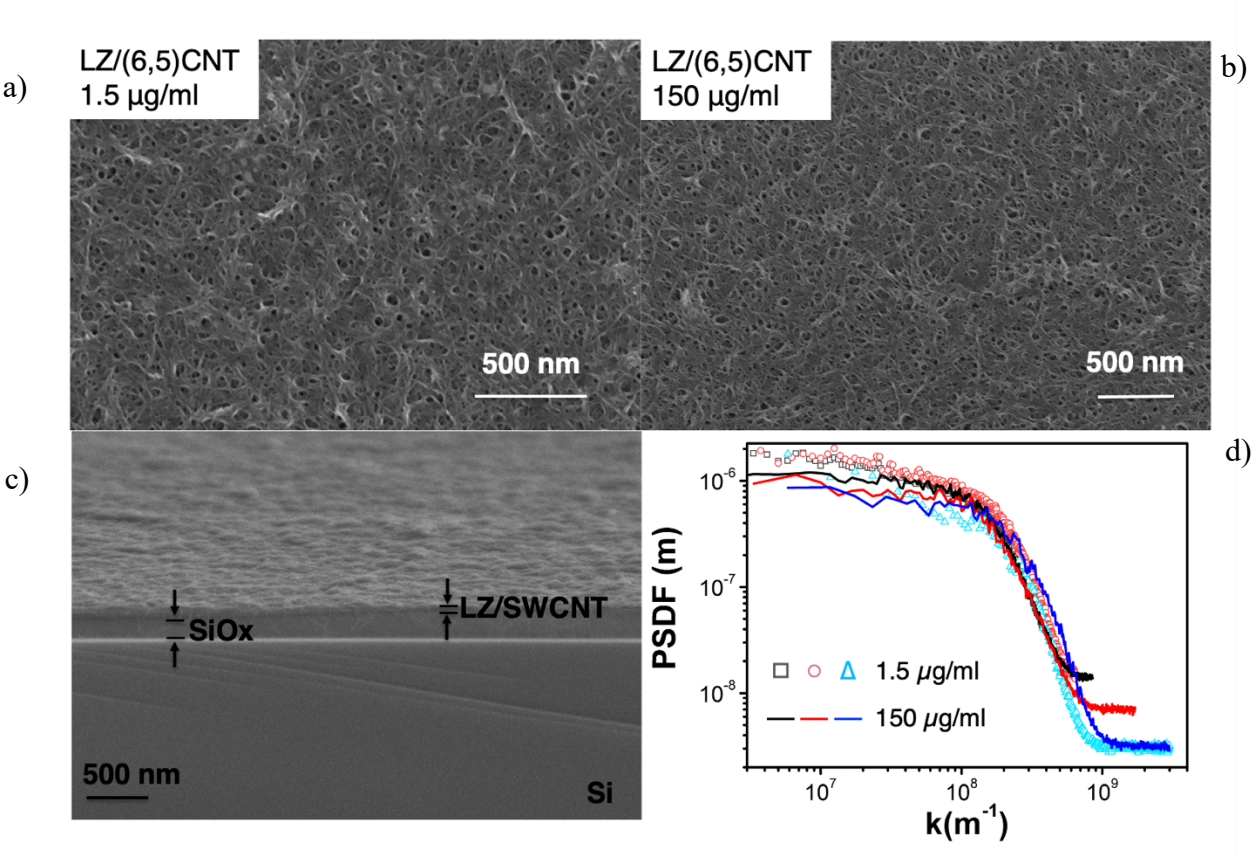

Figure 3. SEM images of LZ/(6,5)CNT networks on Si substrate formed from (a) 1.5 µg/ml solution; (b) 150 µg/ml solution; (c) SEM cross-section of LZ/(6,5)CNT layer on Si test pattern; the Si substrate, the SiO_x dielectric layer and the semiconductive film are visible; (d) PSDF of the images of the LZ/(6,5)CNT networks for 1.5 µg/ml (open symbols) and 150 µg/ml (lines).

Up to this point, we have demonstrated that LZ is an effective dispersive agent for (6,5)CNT, that enables the processing of (6, 5)CNT in aqueous environment. Moreover, the non-covalent lysozyme-(6,5)CNT interaction preserves the semiconducting behavior of the (6,5)CNTs.

For biosensing purposes, it is important to assess that the dispersing protein maintains its functionality. It is well-known that upon interaction with CNTs, lysozyme preserves its activity.[59–61]

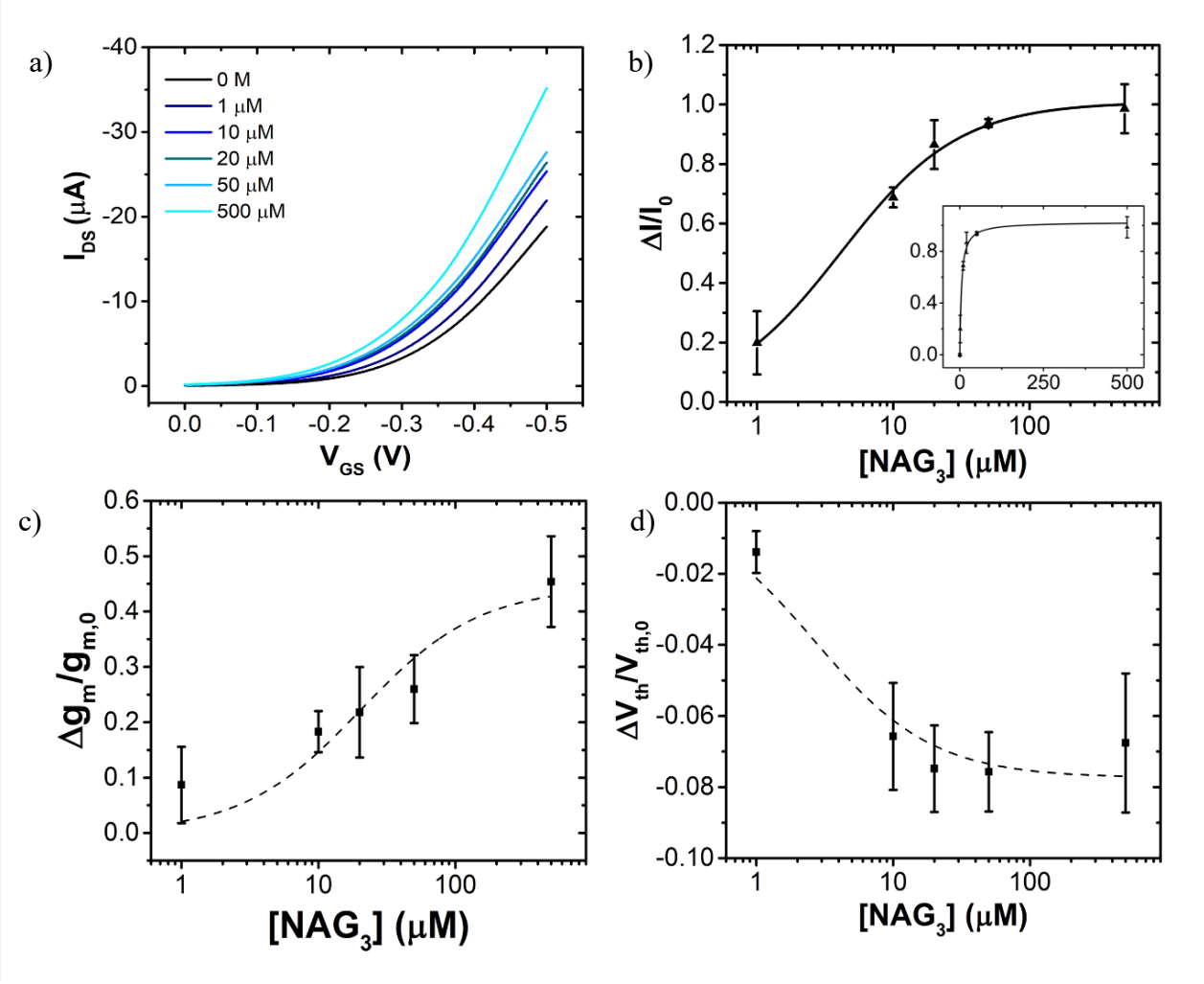

Figure 4. (a) Transfers characteristics upon exposure to different concentrations of NAG_3 (V_{DS} = -0.1 V). NAG_3 concentrations are reported in the inset; (b) biosensor dose curve $\Delta I/I_0$ vs [NAG_3] calculated at gate-source potential V_{GS} = -0.3V. In the inset the dose curves in lin/lin scale; (c) relative variation of transconductance (g_m) and (d) threshold voltage (V_{th})vs NAG_3 concentration. Error bars correspond to the signal averaged over five devices. The data in panel (b), (c) and (d) are fitted with Langmuir equation (equation 1).

In these systems, the control of the spatial orientation of the protein, upon CNT adsorption, is a crucial parameter. If CNTs bind to the catalytic site of the protein, the protein is inhibited.[62]

If the active site of the protein is located away from the interaction area with the CNT, the protein remains active.[44] A docking procedures was used to determine the geometry of the complex formed by LZ and (6,5)CNT. (6,5)CNTs interact with LZ (**Figure S8**), leaving the catalytic site of the protein (made up of the residues Asp52 and Glu35) accessible, suggesting preservation of the full functionality of the protein immobilized on the (6,5)CNTs.

To assess the conservation of lysozyme recognition ability, we used the electrolyte-gated (6,5)CNT transistor as a biosensor to record variations of the electrical response in the presence of increasing concentrations of N-acetyl glucosamine trisaccharide (NAG_3), which is a well-known substrate analogue/inhibitor for this enzyme.[63] The results are reported in **Figure 4**. Transfer characteristics (Figure 4a) change monotonically with the increasing concentration of NAG_3 (from 1 μM to 500 μM); in particular the output current I_{DS} increases when NAG_3 is detected by the transistor.

To minimize device-to-device variability, we build the dose curve that represents the relative average variation of I_{DS}, $\Delta I/I_0$ over five devices at increasing NAG_3 concentrations with respect to the initial current value I_0 (i.e. when no NAG_3 is present in solution).[64] We calculated the curves at different V_{GS} values: the results extracted for V_{GS} = -0.3 V are reported in Figure 4b, where a sigmoidal trend is evident from the best fit curve.

It is also apparent that the transconductance increases and that the transfer curves shift towards more positive values of the threshold voltage, thus mirroring the trend of the relative current variation. These trends are reported in Figures 4c and 4d, respectively. The multiparametric

variation upon exposure to NAG_3 hints to the fact that the interaction between NAG_3 and the enzyme may act both on the Fermi level of the (6,5)CNTs and on the carrier mobility and/or total charge density of the LZ/(6,5)CNT hybrid after interaction with NAG. The subsequent reorganization of the hydration shells and ion distribution in the proximity of the (6,5)CNT bundles would lead to a more effective gating potential, especially when the sensor is operated in the subthreshold regime.[65]

To understand why the device responds so effectively to the presence of NAG_3, we fitted the dose curves with Langmuir model:

$$\left(\frac{\Delta I}{I_0}\right) = \left(\frac{\Delta I}{I_0}\right)_{max} \cdot \frac{K_a[NAG_3]}{1+K_a[NAG_3]} \quad (1)$$

to extract K_a that is the association equilibrium constant of the LZ-NAG_3 pair at the semiconductor/electrolyte interface.

The K_a extracted by fitting the curve in Figure 4b, which was obtained in the subthreshold regime, with the Langmuir model is $(2.1 \pm 0.1)\cdot 10^5$ M^{-1}. As discussed in previous works,[65–70] we notice that the transistor sensitivity (derivative of the device response with respect to [NAG_3] and K_a) depends on the applied V_{GS} (**Figure S9**), although no dramatic changes are observed in the potential window that we investigated (ranging from -0.3 V to -0.5 V), see **Table S2**.

Interestingly, the values of K_a obtained with our LZ/(6,5)CNT transistor biosensor are comparable to the reported values for lysozyme/NAG_3 interaction in solution. In **Table S3** we report the values measured by different technique and expressed as $K_d = 1/K_a$. The K_d value that we obtain at V_{GS} = -0.3 is (4.8 ± 0.3) μM, in line with published values that are invariably in the μM range, although they were obtained with lysozyme and NAG_3 freely diffusing in solution. Compared to other methods for investigating binding thermodynamics, our LZ/(6,5) EGT devices offer a label-free, fast response, with sample volume as low as a few microliters; moreover, they

can be operated without the need for sophisticated instrumentations by simply drop casting the sample solution on the device surface.

3. Conclusion

To conclude, the dispersion of a selected CNT by the lysozyme protein was carried out in water. At odds with other dispersants such as the SDS surfactant, the protein disperses the (6,5)CNT monomolecularly while preserving the electronic properties of the tubes. The solution was drop cast on a silicon substrate where Au source and drain electrodes are interdigitated. The device was first tested as a transistor with the transfer curves of many devices that show remarkably high reproducibility, which is due to the presence of a single type of CNT. Working devices could be obtained even reducing the LZ/(6,5)CNT concentration from 150 μg/ml to 1.5 μg/ml, observing only a moderate worsening of the electrical performances. In particular, the use of a diluted solution yields an increase in the leakage current that we ascribe to higher exposure of the interdigitated S and D electrodes to the electrolyte rather than changes in the semiconducting film morphology. Biorecognition was then demonstrated using increasing concentrations of N-acetyl glucosamine trisaccharide (NAG_3), which is a well-known substrate analogue/inhibitor of lysozyme and found the device to be highly sensitive. Analysis of the device output signal shows that the binding constant of aqueous lysozyme NAG_3 is retained. The present approach is general and can be used to fabricate a new class of highly stable, robust biosensors in a green way in one step from aqueous solutions. We already identified proteins able to interact with CNTs,[38] that can be exploited to fabricate transistors with potential technological applications as sensors for molecules such as nitric oxide (nitric oxide synthase); carbon dioxide (carbonic anhydrase) or urea

(urease), drugs (26-10 FAB:digoxin), natural biomolecules (anti-progesterone antibody) or xenobiotic compounds (cytochrome P450).

ASSOCIATED CONTENT

Supporting Information.

Details of materials and methods; UV-vis absorption spectra and AFM images of Lysozyme and SDS dispersion of (6,5)CNT; electrical characterization of LZ/(6,5)CNT and SDS/(6,5)CNT transistors on silicon and quartz; docking between (6,5)CNT and lysozyme; Kd values for LZ/NAG_3 couple from literature.

AUTHOR INFORMATION

Corresponding Author

* carloaugusto.bortolotti@unimore.it

* matteo.calvaresi3@unibo.it

Author Contributions

The manuscript was written through contributions of all authors. All authors have given approval to the final version of the manuscript.

Funding Sources

FV was partly supported by the Horizon 2020 Framework Programme under the grant FETOPEN-801367 evFOUNDRY. MDG was supported by a FIRC-AIRC fellowship for Italy (id. 22318).

The research leading to these results has received funding from AIRC under MFAG 2019 - ID. 22894 project – P.I. MC. The authors thank PRIN2017-NiFTy (2017MYBTXC) for support.

REFERENCES

[1] J. Wang, *Chem. Rev.* **2007**, *108*, 814.

[2] M. L. Kringelbach, N. Jenkinson, S. L. F. Owen, T. Z. Aziz, *Nat. Rev. Neurosci.* **2007**, *8*, 623.

[3] U. Slawinska, S. Rossignol, D. J. Bennett, B. J. Schmidt, A. Frigon, K. Fouad, L. M. Jordan, *Science (80-.).* **2012**, *338*, 328.

[4] D. Gao, K. Parida, P. S. Lee, *Adv. Funct. Mater.* **2020**, *30*, 1907184.

[5] A. Zhang, C. M. Lieber, *Chem. Rev.* **2016**, *116*, 215.

[6] X. Duan, C. M. Lieber, *Nano Res.* **2015**, *8*, 1.

[7] Z. Yao, C. L. Kane, C. Dekker, *Phys. Rev. Lett.* **2000**, *84*, 2941.

[8] A. Javey, H. Kim, M. Brink, Q. Wang, A. Ural, J. Guo, P. McIntyre, P. McEuen, M. Lundstrom, H. Dai, *Nat. Mater.* **2002**, *1*, 241.

[9] F. Scuratti, J. M. Salazar-Rios, A. Luzio, S. Kowalski, S. Allard, S. Jung, U. Scherf, M. A. Loi, M. Caironi, *Adv. Funct. Mater.* **2020**, 2006895.

[10] T. Dürkop, S. A. Getty, E. Cobas, M. S. Fuhrer, *Nano Lett.* **2004**, *4*, 35.

[11] S. Rosenblatt, Y. Yaish, J. Park, J. Gore, V. Sazonova, P. L. McEuen, *Nano Lett.* **2002**, *2*, 869.

[12] V. Derenskyi, W. Gomulya, J. M. S. Rios, M. Fritsch, N. Fröhlich, S. Jung, S. Allard, S. Z. Bisri, P. Gordiichuk, A. Herrmann, U. Scherf, M. A. Loi, *Adv. Mater.* **2014**, *26*, 5969.

[13] G. Hills, C. Lau, A. Wright, S. Fuller, M. D. Bishop, T. Srimani, P. Kanhaiya, R. Ho, A. Amer, Y. Stein, D. Murphy, Arvind, A. Chandrakasan, M. M. Shulaker, *Nature* **2019**, *572*, 595.

[14] H. Shimotani, S. Tsuda, H. Yuan, Y. Yomogida, R. Moriya, *Adv. Funct. Mater.* **2014**, *24*,

3305.

[15] C. Zhao, D. Zhong, J. Han, L. Liu, Z. Zhang, L. Peng, *Adv. Funct. Mater.* **2019**, *29*, 1808574.

[16] N. Wei, P. Laiho, A. T. Khan, A. Hussain, A. Lyuleeva, S. Ahmed, Q. Zhang, Y. Liao, Y. Tian, E. Ding, Y. Ohno, E. I. Kauppinen, *Adv. Funct. Mater.* **2020**, *30*, 1907150.

[17] G. S. Tulevski, A. L. Falk, *Adv. Funct. Mater.* **2020**, *30*, 1909448.

[18] B. L. Allen, P. D. Kichambare, A. Star, *Adv. Mater.* **2007**, *19*, 1439.

[19] W. S. Wong, A. Salleo, *Flexible Electronics: Materials and Applications*, **2009**.

[20] V. Schroeder, S. Savagatrup, M. He, S. Lin, T. M. Swager, *Chem. Rev.* **2019**, *119*, 599.

[21] H.-E. Jin, C. Zueger, W.-J. Chung, W. Wong, B. Y. Lee, S.-W. Lee, *Nano Lett.* **2015**, *15*, 7697.

[22] X. Xu, P. Clément, J. Eklöf-Österberg, N. Kelley-Loughnane, K. Moth-Poulsen, J. L. Chávez, M. Palma, *Nano Lett.* **2018**, *18*, 4130.

[23] A. Star, J.-C. P. Gabriel, K. Bradley, G. Grüner, *Nano Lett.* **2003**, *3*, 459.

[24] K. Bradley, M. Briman, A. Star, G. Grüner, *Nano Lett.* **2004**, *4*, 253.

[25] H. S. Song, O. S. Kwon, S. H. Lee, S. J. Park, U.-K. Kim, J. Jang, T. H. Park, *Nano Lett.* **2013**, *13*, 172.

[26] T. Murugathas, H. Y. Zheng, D. Colbert, A. V. Kralicek, C. Carraher, N. O. V. Plank, *ACS Appl. Mater. Interfaces* **2019**, *11*, 9530.

[27] Y. Liang, M. Xiao, D. Wu, Y. Lin, L. Liu, J. He, G. Zhang, L.-M. Peng, Z. Zhang, *ACS Nano* **2020**, *14*, 8866.

[28] D. Tasis, N. Tagmatarchis, A. Bianco, M. Prato, *Chem. Rev.* **2006**, *106*, 1105.

[29] R. J. Chen, S. Bangsaruntip, K. A. Drouvalakis, N. Wong Shi Kam, M. Shim, Y. Li, W.

Kim, P. J. Utz, H. Dai, *Proc. Natl. Acad. Sci.* **2003**, *100*, 4984.

[30] A. Antonucci, J. Kupis-Rozmysłowicz, A. A. Boghossian, *ACS Appl. Mater. Interfaces* **2017**, *9*, 11321.

[31] M. Calvaresi, F. Zerbetto, *Acc. Chem. Res.* **2013**, *46*, 2454.

[32] J. López-Andarias, S. H. Mejías, T. Sakurai, W. Matsuda, S. Seki, F. Feixas, S. Osuna, C. Atienza, N. Martín, A. L. Cortajarena, *Adv. Funct. Mater.* **2018**, *28*, 1704031.

[33] J. M. Salazar-Rios, W. Gomulya, V. Derenskyi, J. Yang, S. Z. Bisri, Z. Chen, A. Facchetti, M. A. Loi, *Adv. Electron. Mater.* **2015**, *1*, 1.

[34] N. K. Mehra, V. Mishra, N. K. Jain, *Biomaterials* **2014**, *35*, 1267.

[35] Y. Choi, T. J. Olsen, P. C. Sims, I. S. Moody, B. L. Corso, M. N. Dang, G. A. Weiss, P. G. Collins, *Nano Lett.* **2013**, *13*, 625.

[36] Y. Choi, I. S. Moody, P. C. Sims, S. R. Hunt, B. L. Corso, I. Perez, G. A. Weiss, P. G. Collins, *Science (80-.).* **2012**, *335*.

[37] S. Marchesan, M. Prato, *Chem. Commun.* **2015**, *51*, 4347.

[38] M. Di Giosia, F. Valle, A. Cantelli, A. Bottoni, F. Zerbetto, E. Fasoli, M. Calvaresi, *Carbon N. Y.* **2019**, *147*, 70.

[39] H. J. Salavagione, A. M. Díez-Pascual, E. Lázaro, S. Vera, M. A. Gómez-Fatou, *J. Mater. Chem. A* **2014**, *2*, 14289.

[40] A. S. R. Bati, L. Yu, M. Batmunkh, J. G. Shapter, *Adv. Funct. Mater.* **2019**, *29*, 1902273.

[41] A. M. Münzer, W. Seo, G. J. Morgan, Z. P. Michael, Y. Zhao, K. Melzer, G. Scarpa, A. Star, *J. Phys. Chem. C* **2014**, *118*, 17193.

[42] M. Chen, X. Fu, Z. Chen, J. Liu, W. Zhong, *Adv. Funct. Mater.* **2020**, 2006744.

[43] K. Maehashi, T. Katsura, K. Kerman, Y. Takamura, K. Matsumoto, E. Tamiya, *Anal. Chem.*

2007, *79*, 782.

[44] M. Calvaresi, S. Hoefinger, F. Zerbetto, *Chem. - A Eur. J.* **2012**, *18*, 4308.

[45] R. Contreras-Montoya, G. Escolano, S. Roy, M. T. Lopez-Lopez, J. M. Delgado-López, J. M. Cuerva, J. J. Díaz-Mochón, N. Ashkenasy, J. A. Gavira, L. Álvarez de Cienfuegos, *Adv. Funct. Mater.* **2018**, *29*, 1807351.

[46] H. Gong, F. Chen, Z. Huang, Y. Gu, Q. Zhang, Y. Chen, Y. Zhang, J. Zhuang, Y.-K. Cho, R. H. Fang, W. Gao, S. Xu, L. Zhang, *ACS Nano* **2019**, *13*, 3714.

[47] M. S. Filipiak, M. Rother, N. M. Andoy, A. C. Knudsen, S. Grimm, C. Bachran, L. K. Swee, J. Zaumseil, A. Tarasov, *Sensors Actuators, B Chem.* **2018**, *255*, 1507.

[48] D. Nepal, K. E. Geckeler, *Small* **2006**, *2*, 406.

[49] H. Nie, H. Wang, A. Cao, Z. Shi, S.-T. Yang, Y. Yuan, Y. Liu, *Nanoscale* **2011**, *3*, 970.

[50] M. J. O'Connell, S. M. Bachilo, C. B. Huffman, V. C. Moore, M. S. Strano, E. H. Haroz, K. L. Rialon, P. J. Boul, W. H. Noon, C. Kittrell, J. Ma, R. H. Hauge, R. B. Weisman, R. E. Smalley, *Science,* **2002**, *297*, 593.

[51] W. Gomulya, J. M. S. Rios, V. Derenskyi, S. Z. Bisri, S. Jung, M. Fritsch, S. Allard, U. Scherf, M. C. Dos Santos, M. A. Loi, *Carbon N. Y.* **2015**, *84*, 66.

[52] S. Z. Bisri, J. Gao, V. Derenskyi, W. Gomulya, I. Iezhokin, P. Gordiichuk, A. Herrmann, M. A. Loi, *Adv. Mater.* **2012**, *24*, 6147.

[53] S. Reich, C. Thomsen, P. Ordejón, *Phys. Rev. B* **2002**, *65*, 155411.

[54] W. Kiciński, S. Dyjak, *Carbon N. Y.* **2020**, *168*, 748.

[55] F. Scuratti, G. E. Bonacchini, C. Bossio, J. M. Salazar-Rios, W. Talsma, M. A. Loi, M. R. Antognazza, M. Caironi, *ACS Appl. Mater. Interfaces* **2019**, *11*, 37966.

[56] L. Hu, D. S. Hecht, G. Grüner, *Nano Lett.* **2004**, *4*, 2513.

[57] J. Rivnay, P. Leleux, M. Ferro, M. Sessolo, A. Williamson, D. a. Koutsouras, D. Khodagholy, M. Ramuz, X. Strakosas, R. M. Owens, C. Benar, J.-M. Badier, C. Bernard, G. G. Malliaras, *Sci. Adv.* **2015**, *1*, e1400251.

[58] C. M. Proctor, J. Rivnay, G. G. Malliaras, *J. Polym. Sci. Part B Polym. Phys.* **2016**, *54*, 1433.

[59] D. Nepal, S. Balasubramanian, A. L. Simonian, V. A. Davis, *Nano Lett.* **2008**, DOI 10.1021/nl080522t.

[60] D. W. Horn, K. Tracy, C. J. Easley, V. A. Davis, *J. Phys. Chem. C* **2012**, *116*, 10341.

[61] M. M. Noor, J. Goswami, V. A. Davis, *ACS Omega* **2020**, *5*, 2254.

[62] M. Di Giosia, T. D. Marforio, A. Cantelli, F. Valle, F. Zerbetto, Q. Su, H. Wang, M. Calvaresi, *J. Colloid Interface Sci.* **2020**, *571*, 174.

[63] J. C. Cheetham, P. J. Artymiuk, D. C. Phillips, *J. Mol. Biol.* **1992**, *224*, 613.

[64] F. N. Ishikawa, M. Curreli, H.-K. Chang, P.-C. Chen, R. Zhang, R. J. Cote, M. E. Thompson, C. Zhou, *ACS Nano* **2009**, *3*, 3969.

[65] X. P. A. Gao, G. Zheng, C. M. Lieber, *Nano Lett.* **2010**, *10*, 547.

[66] M. Berto, S. Casalini, M. Di Lauro, S. L. Marasso, M. Cocuzza, D. Perrone, M. Pinti, A. Cossarizza, C. F. Pirri, D. T. Simon, M. Berggren, F. Zerbetto, C. A. Bortolotti, F. Biscarini, *Anal. Chem.* **2016**, *88*, 12330.

[67] C. Diacci, M. Berto, M. Di Lauro, E. Bianchini, M. Pinti, D. T. Simon, F. Biscarini, C. A. Bortolotti, *Biointerphases* **2017**, *12*, 05F401.

[68] M. Berto, C. Diacci, R. D'Agata, M. Pinti, E. Bianchini, M. Di Lauro, S. Casalini, A. Cossarizza, M. Berggren, D. Simon, G. Spoto, F. Biscarini, C. A. Bortolotti, M. Di Lauro, S. Casalini, A. Cossarizza, M. Berggren, D. Simon, G. Spoto, F. Biscarini, C. A. Bortolotti,

Adv. Biosyst. **2018**, *2*, 1700072.

[69] M. Berto, E. Vecchi, L. Baiamonte, C. Condò, M. Sensi, M. Di Lauro, M. Sola, A. De Stradis, F. Biscarini, A. Minafra, C. A. Bortolotti, *Sensors Actuators, B Chem.* **2019**, *281*, 150.

[70] M. Sensi, M. Berto, S. Gentile, M. Pinti, A. Conti, G. Pellacani, C. Salvarani, A. Cossarizza, C. A. Bortolotti, F. Biscarini, *Chem. Commun.* **2021**, *57*, 367.